

## Magnetic Structure of Ni(DCOO)<sub>2</sub>(D<sub>2</sub>O)<sub>2</sub>

Mads R. V. Jørgensen, Mogens Christensen, Mette S. Schmøkel, and Bo B. Iversen\*

Centre for Materials Crystallography, Department of Chemistry and iNANO, Aarhus University, DK-8000 Århus C, Denmark

Received October 1, 2010

Ni(HCOO)<sub>2</sub>(H<sub>2</sub>O)<sub>2</sub> is a structurally simple coordination polymer showing interesting magnetic phase transitions at low temperature (<16K). Previously published studies of these phase transitions have yielded inconsistent results, questioning the correctness of the published magnetic structure. Here heat capacity and magnetic susceptibility of a fully, a partly and a non-deuterated sample were measured, and they all exhibit magnetic phase transitions around 3 and 15 K. Neutron powder diffraction data was collected on the fully deuterated sample at various temperatures between 1.5 and 25 K. A magnetic model was refined against the neutron diffraction data using a spin system composed of two canted antiferromagnetic sublattices. The magnetic moments of the two sublattices show different magnitude, 1.7 μ<sub>B</sub> and 1.3 μ<sub>B</sub>, and the temperature dependence of the magnetic sublattices is quite different. One of the sublattices shows the expected temperature behavior of an antiferromagnetic compound whereas the other sublattice follows a Brillouin like function with a slowly increasing magnetization below the Néel temperature.

### Introduction

Traditionally studies of magnetic properties of materials tend to focus either on inorganic ionic solids (e.g., oxides) or on molecular complexes. In the past decade studies of hybrid materials in the form of extended network structures containing metal centers linked by organic linkers (coordination polymers) have received enormous attention.<sup>1</sup> However, because of the structural complexity of coordination polymers such studies rarely attempt experimental determination of the microscopic magnetic structure, and they primarily focus on measurements of macroscopic magnetic properties.<sup>2,3</sup> One exemption is the transition metal formate dihydrate, M(HCOO)<sub>2</sub>(H<sub>2</sub>O)<sub>2</sub>, which is a comparatively simple coordination polymer. The crystal structure of the isostructural M(HCOO)<sub>2</sub>(H<sub>2</sub>O)<sub>2</sub> compounds has been known since the 1960s, and many studies have focused on their magnetism.<sup>4</sup>

Especially Mn(HCOO)<sub>2</sub>(H<sub>2</sub>O)<sub>2</sub> has been examined since single crystals suitable for neutron scattering experiments can be grown. However, despite these detailed structural studies inconsistencies still exist, and the understanding of the magnetic properties is incomplete. As an example the magnitude of the magnetic moments in the manganese system has been modeled by Radhakrishna et al. using single crystal polarized neutron diffraction data.<sup>5</sup> They found two quite different ions with the magnitudes of the magnetic moments being 0.38(2) μ<sub>B</sub> and 1.73(2) μ<sub>B</sub> for the Mn1 and Mn2 site, respectively. On the other hand, magnetization measurements lead to an overall effective magnetic moment of 5.840(2) μ<sub>B</sub> per ion, which is in good agreement with the free high-spin state of a Mn<sup>2+</sup> ion. This picture was supported by charge density modeling of X-ray diffraction data.<sup>6</sup>

The crystal structure of Ni(HCOO)<sub>2</sub>(H<sub>2</sub>O)<sub>2</sub> is shown in Figure 1, and it belongs to the monoclinic space group *P*2<sub>1</sub>/*c*. The structure contains two distinct Ni ions sites (Ni1 and Ni2) in special crystallographic positions, which are linked by formate groups, and Ni2 is furthermore connected to water molecules, see Figure 1a. The Ni1 ions are coordinated to six formate oxygen atoms forming a slightly distorted octahedron, thereby creating layers in the *bc* planes, see Figure 1b–c. The ions within these layers are interconnected with formate bridges. The Ni2 ions are coordinated to two formate oxygen

\*To whom correspondence should be addressed. E-mail: bo@chem.au.dk. Fax: (+45) 8619 6199.

(1) (a) Chen, B. L.; Xiang, S. C.; Qian, G. D. *Acc. Chem. Res.* **2010**, *43*, 1115. (b) Farah, O. K.; Hupp, J. T. *Acc. Chem. Res.* **2010**, *43*, 1166. (c) Qui, S. L.; Zhu, G. S. *Coord. Chem. Rev.* **2009**, *253*, 2891. (d) Wang, Z. Q.; Cohen, S. M. *Chem. Soc. Rev.* **2009**, *38*, 1315. (e) Lee, J.; Farah, O. K.; Roberts, J.; Scheidt, K. A.; Nguyen, S. T.; Hupp, J. T. *Chem. Soc. Rev.* **2009**, *38*, 1450. (f) Li, J. R.; Kuppler, R. J.; Zhou, H. C. *Chem. Soc. Rev.* **2009**, *38*, 1477. (g) Robin, A. Y.; Fromm, K. M. *Coord. Chem. Rev.* **2006**, *250*, 2127. (h) Kitagawa, S.; Kitaura, R.; Noro, S. I. *Angew. Chem., Int. Ed.* **2004**, *43*, 2334.

(2) Poulsen, R. D.; Bentien, A.; Chevalier, M.; Iversen, B. B. *J. Am. Chem. Soc.* **2005**, *50*, 9156.

(3) Clausen, H. F.; Overgaard, J.; Chen, Y.-S.; Iversen, B. B. *J. Am. Chem. Soc.* **2008**, *64*, 7988.

(4) (a) Osaki, K.; Nakai, Y.; Watanabe, T. *J. Phys. Soc. Jpn.* **1964**, *19*, 717. (b) Osaki, K.; Nakai, Y.; Watanabe, T. *J. Phys. Soc. Jpn.* **1963**, *18*, 919.

(5) Radhakrishna, P.; Gillon, B.; Chevrier, G. *J. Phys.: Condens. Matter* **1993**, *5*, 6447.

(6) Poulsen, R. D.; Jørgensen, M. R. V.; Overgaard, J.; Larsen, F. K.; Morgenroth, W. G.; Graber, T.; Chen, Y.-S.; Iversen, B. B. *Chem.—Eur. J.* **2007**, *13*, 9775.

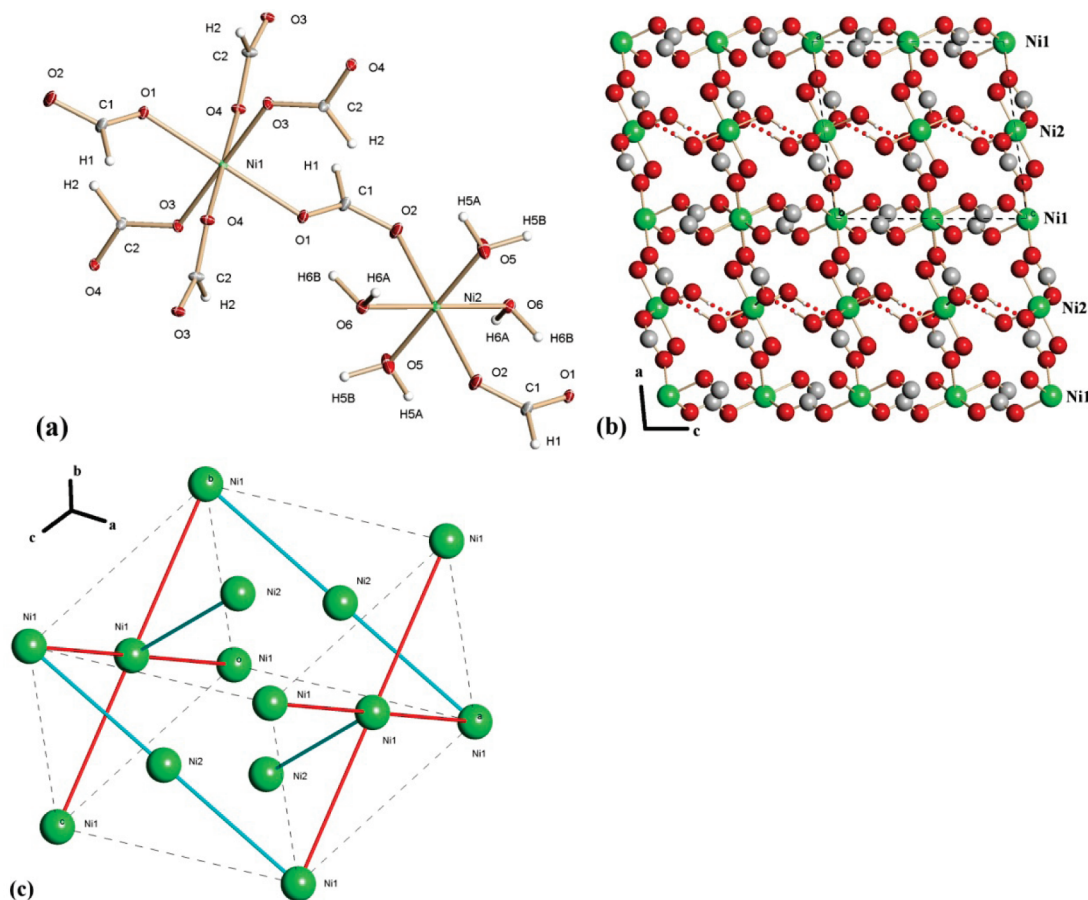


**Figure 1.** (a) Structure of  $\text{Ni}(\text{HCOO})_2(\text{H}_2\text{O})_2$  at 100 K with thermal ellipsoids shown at 50% probability level. (b) The structure viewed along the monoclinic  $b$ -axis. The  $\text{H5B}\cdots\text{O2}$  hydrogen bonds are shown using dotted bonds. (c) Unit cell showing only Ni atoms and schematic “formate” connections.

atoms and four water ligands, also in a slightly distorted octahedral geometry. The water ligands in the equatorial plane of the coordination sphere of Ni2 provide only electrostatic interactions between the Ni2 centers and thus efficiently disconnect the Ni2 ions within these layers that interpenetrate the layers formed by the Ni1 ions. The two different layers are connected by formate bridges between Ni1 and Ni2 creating a three-dimensional (3D) network. In this network the Ni1 ions are connected through covalent bonds while the Ni2 ions are virtually isolated from each other. In the crystal structure there are four reasonably strong hydrogen bonds formed by the water hydrogen atoms. Three of these four hydrogen bonds are from the water in the Ni2 layer to the Ni1 layer while the last (connecting H5B to O2) is within one Ni2 layer. The latter hydrogen bond thus leads to a more “direct” interaction between neighboring Ni2 ions, Figure 1b.

The magnetic ordering of  $\text{Ni}(\text{HCOO})_2(\text{H}_2\text{O})_2$  was reported to consist of an antiferromagnetic ordering of Ni1 moments ( $\mu_1$ ) at  $T_N = 15.5$  K while the moments on Ni2 ( $\mu_2$ ) behave almost paramagnetic until sublattice antiferromagnetic ordering at  $T = 3$  K.<sup>7,8</sup> In the manganese analogue, Pierce and Friedberg noted, that the magnetic ordering in the Mn1 sublattice necessarily has to involve a finite ordering of the Mn2 sublattice. This ordering, however, is small and thus the Brillouin function is small. This leads to moments that

behave nearly as in a paramagnetic system.<sup>9</sup> Kageyama et al. has recently reported a molecular-field model that also shows a similar small ordering of the Ni2 sublattice at the overall Néel temperature.<sup>10</sup>

$\text{Ni}(\text{HCOO})_2(\text{H}_2\text{O})_2$  has been studied with a broad range of methods such as magnetization and magnetic susceptibility,<sup>8,10</sup> specific heat capacity,<sup>7,11</sup> and neutron powder diffraction.<sup>12</sup> More recently, the compound was studied by proton NMR by Zenmyo et al.<sup>13</sup> There are discrepancies between results obtained with different methods. Magnetic susceptibility measurements and neutron diffraction suggest  $\mu_{\text{eff}} = 3.14 \mu_B$  and  $\mu_1 = \mu_2 \sim 2.0(2) \mu_B$ , respectively. The spin model presented by Zenmyo et al. based on NMR measurements suggests  $\mu_1 = 2.38 \mu_B$  and  $\mu_2 = 0.38 \mu_B$ , and this is in agreement with the weak ferrimagnetism observed by Kageyama et al.<sup>10</sup> The NMR model also seems to explain the compensation point observed by the same authors.<sup>10</sup> The moments reported by Zenmyo et al. raise the question why  $\mu(\text{Ni1}) > \mu(\text{Ni2})$  when  $\mu(\text{Mn2}) > \mu(\text{Mn1})$  in the isostructural manganese analogue. If this is the case then the chemical

(7) Pierce, R. D.; Friedberg, S. A. *Phys. Rev. B* **1971**, *3*, 934.

(8) Hoy, G. R.; Barros, S. D. S.; Barros, F. D. S.; Friedberg, S. A. *J. Appl. Phys.* **1965**, *36*, 936.

(9) Pierce, R. D.; Friedberg, S. A. *Phys. Rev.* **1968**, *165*, 680.

(10) Kageyama, H.; Khomskii, D. I.; Levitin, R. Z.; Vasil'ev, A. N. *Phys. Rev. B* **2003**, *67*, 224422.

(11) Takeda, K.; Kawasaki, K. *J. Phys. Soc. Jpn.* **1971**, *31*, 1026.

(12) Burllet, P.; Burllet, P.; Rossatmignod, J.; Decornbarieu, A.; Bedin, E. *Phys. Status Solidi B* **1975**, *71*, 675.

(13) Zenmyo, K.; Kubo, H.; Tokita, M.; Yamagata, K. *J. Phys. Soc. Jpn.* **2006**, *75*, 104704.

bonding in the coordination polymer must play a central role in determining the magnetic properties.

The compound  $\text{Ni}(\text{HCOO})_2(\text{H}_2\text{O})_2$  does not grow sufficiently large single crystals for a single crystal neutron diffraction experiment. Therefore, the present neutron study concerns a powder sample, but this leads to complications because of the relative high hydrogen content of the material, which causes a high incoherent background. To improve the signal-to-noise ratio the neutron study was carried out on a deuterated sample. A total of three samples, a fully, a partly and a non-deuterated sample, were synthesized. Measurements of the heat capacity and the magnetic susceptibility were carried out on all three samples to assess the similarity between the deuterated and the fully hydrogenated compounds.

## Experimental Section

**Synthesis.** The sample used in both the neutron diffraction experiments and the measurements of the physical properties was grown at the interface between a layer of deuterated formic acid and a layer of Ni-acetate in a mixture of heavy water ( $\sim 100\%$  pure) and ethanol. Hydrogen contamination from the atmosphere was avoided by carrying out the reaction in an inert  $\text{N}_2$  atmosphere. The synthesis produced a powder consisting of small green crystals. A partly deuterated sample was prepared using the same approach but using “regular” hydrogenated formic acid and heavy water ( $\sim 100\%$  pure). Finally, a fully hydrogenated sample was prepared using hydrogenated formic acid and water. During the synthesis it was observed that the crystallization of the deuterated compounds was slower than the synthesis using regular “light” water. Powder X-ray diffraction confirmed that the prepared compounds were the title compound and that the samples were phase pure.

**Physical Properties Measurement.** The magnetic susceptibility measurements were carried out on small pellets of pressed powder. A Quantum Design Physical Property Measurement System (PPMS) at the Department of Chemistry, Aarhus University, was used in the temperature range from 1.9 K to room temperature in a field of 2 T to measure the magnetic susceptibility. The same sample batch was used for the magnetic susceptibility and the subsequent neutron powder diffraction experiments. During the measurement of the magnetic susceptibility of the partly deuterated sample there were some problems with the gain amplification leading to systematically lower values of the magnetic susceptibility. Consequently, the magnetic susceptibility of the partly deuterated sample was scaled linearly to the magnetic susceptibility of the deuterated sample using the temperature interval 50 to 250 K. Measurements of the heat capacity were also performed with the PPMS. Small pellets of the three samples were mounted on the sample holder with a small amount of grease. The amount of grease used in the measurement of the heat capacity of the deuterated sample was unfortunately erroneous, thus leading to an incorrect addenda signal subtraction. Therefore the addenda signal, that is, the mass of grease, has been rescaled.

**Neutron Powder Diffraction.** The neutron diffraction experiments were performed at the quasi-continuous neutron spallation source (SINQ) at the Paul Scherrer Institute (PSI) in Villigen, Switzerland. The sample was handled in a He containing glovebox, where it was ground in a mortar to avoid preferential orientations of crystallites. The powder was transferred to a 6 mm vanadium cylinder, which was sealed using a piece of indium wire. The helium gas in the sample container acts as protecting atmosphere and heat exchanger. The sample was transferred to a helium cryostat (Orange ILL type) at the DMC neutron powder diffractometer located at the cold neutron source. This instrument is equipped with a banana-shaped position sensitive

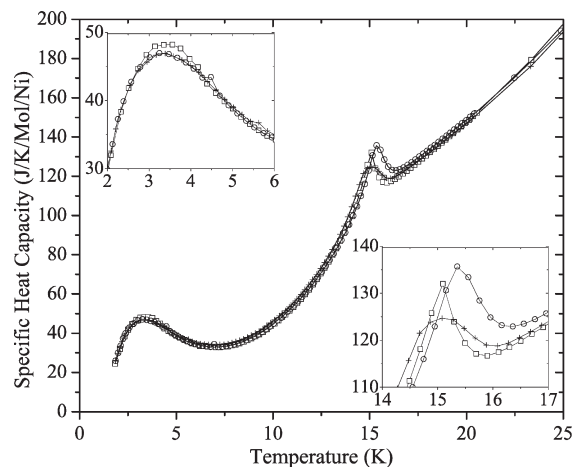


**Figure 2.** Specific heat capacity of the samples with circles (○) for the hydrogenated sample, plus symbols (+) for the partly deuterated sample, and squares (□) for the fully deuterated sample. The lines are guides to the eye. Insets show peaks close up.

detector covering  $80^\circ$  with 400 channels at  $0.2^\circ$  interval, and successive powder diffraction patterns were collected with  $0.1^\circ$  steps to improve peak resolution.<sup>14</sup> Diffraction patterns at low  $Q$  with good statistics were recorded at 25, 6, and 1.5 K, that is, above, in-between, and below the two phase transitions. These patterns were recorded at two different wavelengths of 2.45 Å and 4.2 Å using a vertical focusing (002) graphite monochromator. Furthermore, a series of patterns with less precise statistics were recorded stepping up in temperature in small intervals. To prevent any hysteresis effects<sup>10</sup> the desired temperature was always reached by cooling from above 25 K to the lowest possible temperature ( $\sim 1.5$  K) and then reheating to the desired temperature.

After the DMC measurements the sample was transferred to the HRPT instrument and placed in a similar helium cryostat to record the high- $Q$  region of the powder diffraction pattern. The HRPT instrument is located at the hot neutron source, and it is equipped with a banana-shaped detector covering  $160^\circ$  with 1600 channels at  $0.1^\circ$  intervals, and successive powder diffraction patterns were collected with  $0.05^\circ$  steps to improve peak resolution.<sup>15</sup> Three diffraction patterns were recorded at 1.5, 6, and 25 K using neutrons with a wavelength of 1.89 Å obtained from a vertically focusing (511) Ge monochromator. Neutron diffraction data were only measured using the fully deuterated sample.

## Results and Discussion

**Physical Property Measurements.** The signatures of the two phase transitions are easily seen in the heat capacity, Figure 2. The change in heat capacity at low temperature  $\sim 3.5$  K is assumed to be associated with the complete magnetic ordering of the  $\text{Ni}_2$  sublattice. This phase transition is close to identical for the three samples, while the second peak differs slightly between the three samples. The two samples containing heavy water are shifted toward lower temperature,  $\sim 15.1$  K, with respect to the fully hydrogenated sample,  $\sim 15.4$  K, and the shape of the peak is also different. The fully deuterated and fully

(14) Fischer, P.; Keller, L.; Schefer, J.; Kohlbrecher J. *Neutron News* **2000**, *11*, 19.

(15) Fischer, P.; Frey, G.; Koch, M.; Könnecke, M.; Pomjakushin, V.; Schefer, J.; Thut, R.; Schlumpf, N.; Bürge, R.; Greuter, U.; Bondt, S.; Berruver, E. *Physica B* **2000**, *276–278*, 146.

**Table 1.** Refinement Residual Factors for the HRPT Data at 1.89 Å (I), the DMC Data at 4.2 Å (II), and the DMC Data at 2.45 Å (III)<sup>a</sup>

	25 K			6 K			1.5 K			1.5 K NMR model		
	I	II	III	I	II	III	I	II	III	I	II	III
no. of reflections	682	42	145	1369	88	251	1369	88	293	1369	88	293
no. of parameters	88	88	88	47	47	47	68	68	68	65	65	65
$R_F$	3.19	1.97	1.71	3.33	1.35	1.53	3.02	1.24	1.68	3.02	1.61	1.82
$R_{wp}$	10.7	5.92	5.49	11.8	5.63	5.91	10.4	5.12	6.17	10.8	8.43	7.62
$R_p$	10.0	6.41	5.45	11.1	5.81	5.82	9.93	5.32	6.11	10.3	7.60	7.05
$R_{Bragg}$	5.03	1.96	2.15	5.33	1.83	2.40	4.70	1.34	2.49	4.70	1.50	2.79
$R_{Mag}$	N/A	N/A	N/A	21.1	8.55	13.5	14.9	7.27	7.16	51.7	78.7	60.1
$\chi^2$	10.1			11.7			11.8			22.4		

<sup>a</sup> The agreement factors are defined by  $R_p = \sum |y_{o,i} - y_{c,i}| / \sum |y_{o,i}|$ ,  $R_{wp} = [\sum w_i |y_{o,i} - y_{c,i}|^2 / \sum w_i |y_{o,i}|^2]^{1/2}$ ,  $\chi^2 = \sum w_i |y_{o,i} - y_{c,i}|^2 / \sigma_i^2$ ,  $R_F = \sum |F_o - F_c| / \sum |F_o|$ ,  $R_{mag}$  is similar to  $R_F$  but for the magnetic peaks.

hydrogenated samples both show sharp peaks, while the partly deuterated sample shows a broad round peak.

The heat capacity is very similar to the values reported in the literature for hydrogenated samples.<sup>7,11</sup> The round peak found for the partly deuterated sample at 15 K is similar to the previously reported shapes, whereas it is the sharper peaks of the fully deuterated and fully hydrogenated samples that differ. We currently have no explanation for this difference. The shift of the peak position could indicate that the hydrogen bonds in the structure may be involved in the magnetic ordering as proposed by Poulsen et al.<sup>6</sup>

From the magnetization measurements the magnetic susceptibility was calculated and the paramagnetic region from approximately 50 to 270 K was fitted with the Curie–Weiss law. Quite similar values for the effective moment ( $\mu_{eff}$ ) were calculated for the three samples, 2.88(1)  $\mu_B$ , 2.89(1)  $\mu_B$ , and 3.03(1)  $\mu_B$  for the fully deuterated, the partly deuterated, and the fully hydrogenated sample, respectively, and the Weiss temperatures ( $\Theta$ ) were found to be -12.1(2), -12.7(1), and -9.1(5) K. Nevertheless, the data may indicate a slight difference between the deuterated and the hydrogenated samples. In a similar experiment Kageyama et al. reported values for  $\mu_{eff}$  (3.14  $\mu_B$ ) and  $\Theta$  (-15.5 K).<sup>10</sup> The value for the effective magnetic moment is close to, but exceeds, the spin only value of a free Ni<sup>2+</sup> ion; 2.82  $\mu_B$ . Although the effective magnetic moment of the hydrogenated sample is higher and the Weiss temperature lower than the values obtained from the measurements on the deuterated samples, it appears that the magnetic ordering in the deuterated sample is similar to the magnetic ordering in the hydrogenated sample.

**Magnetic Structure.** The magnetic and structural models were simultaneously refined against the two DMC data sets and the HRPT data set using the Rietveld method implemented in the FullProf program.<sup>16,17</sup> The starting model was obtained from highly accurate single crystal synchrotron X-ray diffraction data measured at 100 K (unpublished results). The structural model was refined against the three 25 K data sets, and all positions, isotropic displacement parameters, and peak profiles were included in the refinement. Furthermore, the occupancies of the hydrogen/deuterium positions were refined. It was found that the deuterium occupancy on the formate

**Table 2.** Components and Magnitudes of the Magnetic Moments at 1.5 and 6 K

	$\mu_1(x)/\mu_B$	$\mu_1(y)/\mu_B$	$\mu_1(z)/\mu_B$	$ \mu_1 /\mu_B$	$\mu_2(x)/\mu_B$	$\mu_2(y)/\mu_B$	$\mu_2(z)/\mu_B$	$ \mu_2 /\mu_B$
1.5 K	1.2(1)	0.4(3)	-1.0(2)	1.7(3)	0.4(1)	0 <sup>a</sup>	-1.2(2)	1.3(2)
6 K	0.8(1)	0.5(3)	-1.5(2)	1.7(2)	0 <sup>a</sup>	0 <sup>a</sup>	-0.7(1)	0.7(1)

<sup>a</sup> These components were removed from the model because of unreliable refinement of the values.

groups was 100% and that the deuterium occupancies on the water sites were close to 90%. This structural model was subsequently used as a starting model in the refinement of the magnetic phases.

The 1.5 and 6 K phases were modeled by adding a magnetic phase to the 25 K structural model. The magnetic model consisted of two canted antiferromagnetic sublattices with both sublattices canted in the *b* direction. All non-hydrogen atom positions and peak profiles were refined while the positions and occupancies of the hydrogen/deuterium atoms along with all displacement parameters were kept at the values obtained from the 25 K data. The magnetic phase was modeled in space group  $P\bar{1}$  after a representational analysis performed in the program SARAh.<sup>18</sup>

The general assumption regarding the magnetic ordering is that the Ni1 lattice orders at 15.5 K while the Ni2 lattice only shows small ordering and can therefore be approximated as “paramagnetic” down to ~3 K. Therefore, the initial 6 K model did not include  $\mu_2$ . However, addition of this moment significantly improved the fit, and it was therefore included in the final model. Refinement details from the final models are shown in Table 1. A comparison of the two different 6 K models can be found in the Supporting Information.

Although the refinements in general were stable, the refinement of the magnetic moment along the *b* axis was unstable because of its small value (~0.1–0.2  $\mu_B$ ), and it was therefore omitted from the Ni2 sublattice at both 1.5 and 6 K. Similarly, the Ni2 moment along the *a* axis had to be removed from the 6 K model as this also was too small to be modeled reliably. During the refinements it was noted that the absolute direction of the moment could be changed to the directly opposite direction causing only a very small change in the *R*-values and no visual change in the fit to the data. This is presumably due to the rather weak signal of the magnetic scattering compared with the nuclear scattering combined with the small

(16) Rietveld, H. M. *Aust. J. Phys.* **1988**, *41*, 113.

(17) Rodriguezcarvajal, J. *Phys. B* **1993**, *192*, 55.

(18) Wills, A. S. *Phys. B* **2000**, *276*, 680.

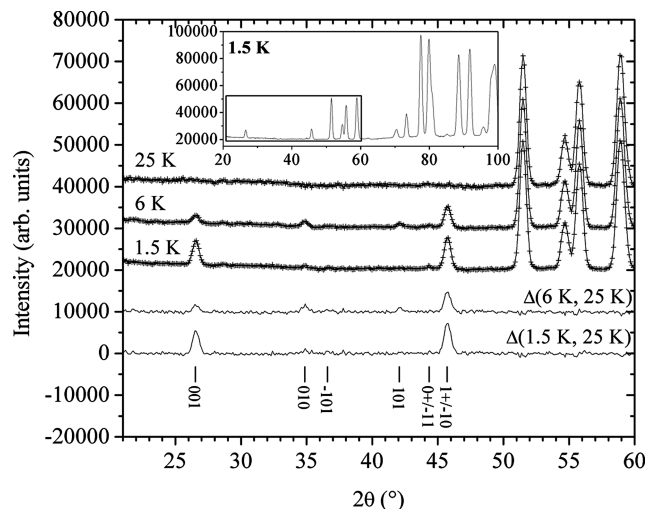


**Figure 3.** Diffraction data from DMC at 4.2 Å. From top: 25, 6, 1.5 K, difference between 6 and 25 K, and difference between 1.5 and 25 K. Vertical lines show Bragg positions. The inset shows the full diffractogram, and the box indicates the region of interest. The diffraction patterns are offset for clarity.

deviation from orthorhombic symmetry ( $\beta \sim 97^\circ$ ). The directions presented here (see Table 2 and Figure 4) are the ones that gave the lowest agreement factors. The low angle 1.5, 6, and 25 K data from DMC, along with the difference between data and models, are shown in Figure 3. Selected Rietveld fits are included in the Supporting Information.

The magnitude of the moments at 1.5 K were found to be  $1.7(3) \mu_B$  and  $1.3(2) \mu_B$  for Ni1 and Ni2, respectively. At 6 K the values were refined to  $1.7(2) \mu_B$  and  $0.7(1) \mu_B$ . The components of the moments are given in Table 2 and shown in Figure 4. To compare the present magnetic model with the NMR model proposed by Zenmyo et al.<sup>13</sup> the reported moments from the NMR study were added at fixed values to the structural model, while the atomic parameters, unit cell and background were refined. This model leads to very high  $R$ -values (see Table 1), and the corresponding Rietveld fit is shown in Figure 5.

**Temperature Dependence of the Magnetic Moments.** The temperature dependence of the magnetic moments was modeled using data collected on the DMC instrument. For the temperatures in the range 1.5 to 12 K, the magnetic model was refined against data collected using both 2.45 Å and 4.2 Å neutrons, whereas the model in the temperature range 13 to 15.5 K only was refined against 4.2 Å data (2.45 Å data was not collected in this temperature range). In these models only the background, the unit cell, and the magnetic moments were refined. As described above, a significant moment on Ni2 was found at 6 K. Similar improvements of the fits at higher temperature than 6 K was also observed, and the model including  $\mu_2$  was chosen as the most reliable. Adding  $\mu_2$  to the model does not change the magnitude of  $\mu_1$  significantly. The temperature dependence of the magnetic moment on the two sites is shown in Figure 6. The moments obtained at 1.5 and 6 K using all data (DMC, 2.45 Å and 4.2 Å, and HRPT at 1.89 Å), are also shown in this figure.

As seen from Figure 6, the temperature dependence of  $\mu_1$  shows the expected temperature dependence of an ordering of magnetic spins with a rapid decrease as the

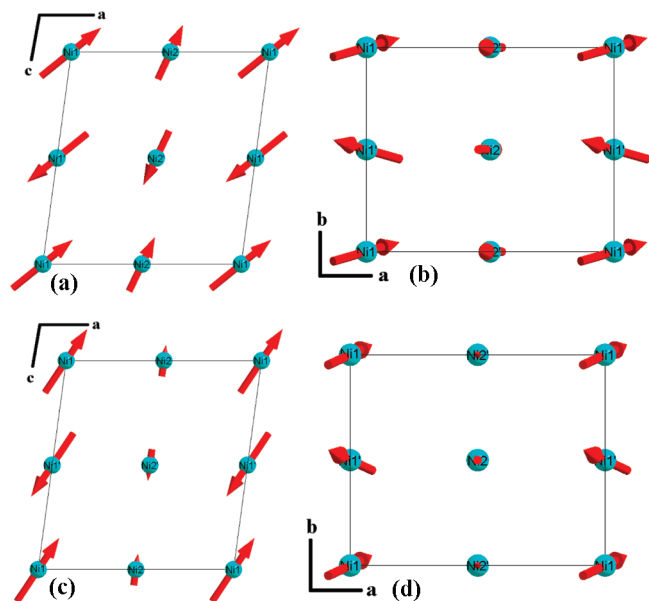


**Figure 4.** Projections of the unit cell showing the magnetic moments. (a) 1.5 K, projection along  $b$ . (b) 1.5 K, projection along  $c$ . (c) 6 K, projection along  $b$ . (d) 6 K, projection along  $c$ .

temperature approaches the Néel temperature (15.5 K). On the other hand  $\mu_2$  deviates from this behavior and shows a Brillouin like behavior resulting in a small and slowly decreasing moment in a large temperature range. A similar result has been reported in the literature based on molecular-field modeling.<sup>9,10</sup> The agreement between that model and the present results is quite good for the Ni1 sublattice magnetization. When comparing the Ni2 sublattice magnetization it is seen that the molecular-field model overestimates the  $\mu_2$  ordering in the temperature range from  $\sim 4$  K to  $\sim 13$  K. This could be due to a too simplified model ignoring the Ni2–Ni2 interaction or simply a slightly wrong estimate of the Ni1–Ni2 exchange parameter. The temperature dependence of the Ni2 sublattice magnetization is presumably due to the magnetic field from the Ni1 layers, the exchange with the Ni1 layers, and the weak interaction in the Ni2 layer. This is also reflected in the molecular-field models.

As noted above the model reported by Zenmyo et al. based on NMR measurements gave a poor fit to the neutron data (Figure 5). The two models differ not only on the direction of the moments but also on the magnitude. Despite these differences they both describe an antiferromagnetic ordering in the  $ac$  planes with canting in the  $b$  direction. The magnetic moment along the  $b$  axis, because of canting, is quite similar. Compared with the results obtained from magnetic susceptibility measurements it seems that both NMR and neutron scattering underestimates the moments. However, it is not straightforward to compare these values as the magnetization is measured in the paramagnetic regime whereas NMR and neutron measurements are performed in the ordered state. The moments obtained from the ordered state will be smaller than the ones obtained from the paramagnetic state because of temperature fluctuations of the moments. Figure 6 indicates that  $\mu_1$  has saturated and that  $\mu_2$  is close to saturation. The estimated average moment or effective moment obtained from NMR is  $1.4 \mu_B$ , and it is  $1.5 \mu_B$

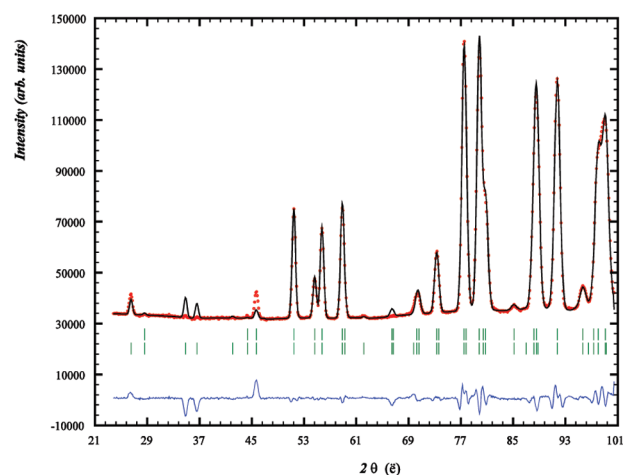
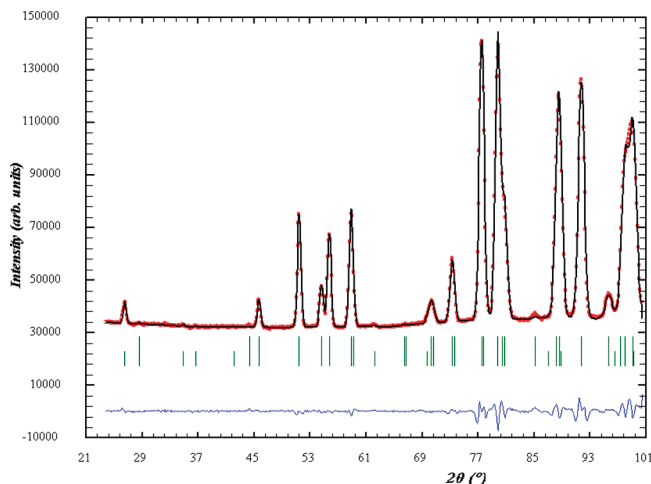


**Figure 5.** Rietveld fit of 1.5 K data measured at DMC with 4.2 Å neutrons using (left) the present model and (right) the magnetic model proposed by Zenmyo et al. The red dots show the measurements, the black line shows the model, and the blue line shows the difference. Green bars show predicted Bragg positions. The upper green bars show predicted Bragg positions for the structure while lower bars show predicted Bragg positions for the magnetic phase.

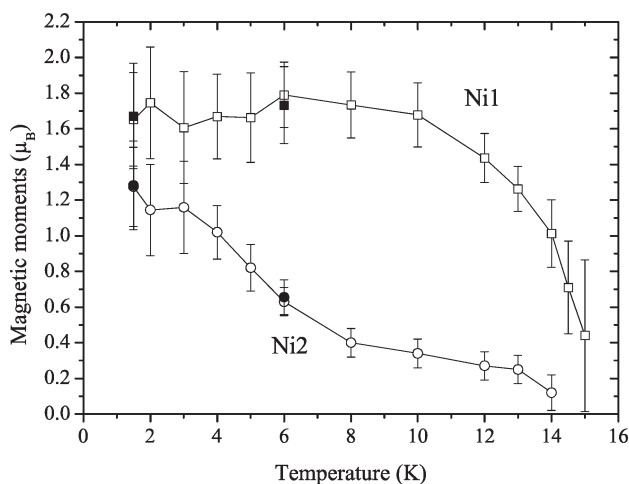


**Figure 6.** Temperature dependence of the magnitude of the magnetic moment of Ni1 (open squares) and Ni2 (open circles). The closed squares and closed circles represent the magnitude of the Ni1 and Ni2 moments obtained from all available data sets.

from the present neutron study. This is approximately 50% of the effective moment obtained from magnetization measurements.

## Conclusions

On the basis of heat capacity measurements it is concluded that the magnetic ordering in  $\text{Ni}(\text{DCOO})_2(\text{D}_2\text{O})_2$  is similar to that observed in the regular hydrogenated compound,  $\text{Ni}(\text{HCOO})_2(\text{H}_2\text{O})_2$ . The magnetic structure is composed of

two canted antiferromagnetic sublattices leading to a weak ferrimagnet. The magnitude of the magnetic moments at 1.5 K is found to be  $1.7(2)\mu_{\text{B}}$  and  $1.3(2)\mu_{\text{B}}$  for Ni1 and Ni2, respectively, which is much lower than the free  $\text{Ni}^{2+}$  ion value, and significantly lower than the value obtained from magnetization measurements. The temperature dependence of the sublattices is in good agreement with the molecular-field model suggested in the literature and shows the small but significant ordering of the Ni2 sublattice at the Neel temperature of the Ni1 sublattice. The magnetic model presented here has weak ferrimagnetism created by two canted antiferromagnetic sublattices. The canting is along the  $b$  axis, and the resulting moments of the two sublattices are opposed.

**Acknowledgment.** We gratefully acknowledge and fondly remember the assistance of recently deceased Marie Agnes Chevallier during synthesis of the materials. Dr. L. Keller and Dr. D. Sheptyakov are thanked for assistance during the neutron measurements. This work is based on experiments performed at the Swiss spallation neutron source SINQ, Paul Scherrer Institute, Villigen, Switzerland. The work was supported by The Danish National Research Foundation (Center for Materials Crystallography), The Danish Strategic Research Council (Centre for Energy Materials), and the Danish Research Council for Nature and Universe (Danscatt).

**Supporting Information Available:** Magnetic susceptibility data, specific heat capacity data, and Rietveld refinement plots. This material is available free of charge via the Internet at <http://pubs.acs.org>.